

Intravital imaging of amyloid plaques in a transgenic mouse model using optical-resolution photoacoustic microscopy

Song Hu,^{1,†} Ping Yan,^{2,†} Konstantin Maslov,¹ Jin-Moo Lee,^{2,3} and Lihong V. Wang^{1,4}

¹Department of Biomedical Engineering, Washington University in St. Louis, St. Louis, Missouri, USA

²Department of Neurology and the Hope Center for Neurological Disorders, Washington University School of Medicine, St. Louis, Missouri, USA

³leejm@neuro.wustl.edu

⁴lhwang@biomed.wustl.edu

Received July 8, 2009; revised November 10, 2009; accepted November 10, 2009; posted November 12, 2009 (Doc. ID 114001); published December 15, 2009

We report optical-resolution photoacoustic microscopy (OR-PAM) for *in vivo* imaging of amyloid plaques in an Alzheimer's disease mouse model. Validation using conventional fluorescence microscopy and multiphoton microscopy shows that OR-PAM has sufficient sensitivity and spatial resolution to identify amyloid plaques in living brains. In addition, with dual-wavelength OR-PAM, the three-dimensional morphology of amyloid plaques and the surrounding microvasculature are imaged simultaneously through a cranial window without angiographic contrast agents. OR-PAM, capable of providing both exogenous molecular contrast and endogenous hemoglobin contrast, has the potential to serve as a new technology for *in vivo* microscopic observations of cerebral plaque deposits. © 2009 Optical Society of America
OCIS codes: 170.3880, 170.5120, 170.6900.

Amyloid- β , the primary constituent of senile plaques, is hypothesized to play a major role in the pathogenesis of Alzheimer's disease (AD), but the underlying mechanisms are still elusive. Recent advances in established clinical imaging modalities have permitted noninvasive imaging of amyloid deposits in patients [1]. However, the neuropathologic changes in AD are microscopic, and subtle changes due to disease progression or treatment may be undetectable by such clinical instruments because of their low spatial resolutions. Multiphoton microscopy, a commercially available laser-scanning microscopy technique, allows imaging of amyloid plaques with high sensitivity and submicrometer resolution in animal models [2]. However, its applications are limited by the inability to image through the intact skull, thereby requiring cranial window preparations.

Here, we report the first application of optical-resolution photoacoustic microscopy (OR-PAM) toward imaging amyloid plaques in an AD transgenic mouse model. OR-PAM images of Congo-red-stained brain sections from these mice were virtually identical to fluorescence images. Moreover, *in vivo* OR-PAM images through a cranial window also showed high correlation with observations by multiphoton microscopy. As a new technology for *in vivo* amyloid plaque imaging, OR-PAM provides both the exogenous molecular contrast from the amyloid-specific Congo red dye and the endogenous absorption contrast from hemoglobin, enabling simultaneous visualization of cerebral microvasculature without using angiographic dye.

Figure 1 shows a schematic of the OR-PAM system for intravital amyloid plaque imaging. To maximize the imaging sensitivity, optical illumination and ultrasonic detection in our OR-PAM system are configured confocally by an acoustic-optical beam splitter [3]. The beam splitter is nearly transparent to the op-

tical illumination, but the oil-glass surface at the diagonal reflects almost all the ultrasonic signals to a 75 MHz ultrasonic transducer [V2022 (BC), Olympus NDT] attached to the vertical side of the bottom prism. The near-diffraction-limited optical focusing achieved by a commercial microscope objective (RMS4 \times , Thorlabs) determines the 5 μm lateral resolution of OR-PAM. An acoustic lens (NA 0.46) is attached to the bottom of the beam splitter and immersed in a water tank to collect photoacoustic signals. A window is opened in the bottom of the water tank and sealed with an ultrasonically and optically transparent polyethylene membrane to expose the imaging site. For simplification, the water tank is not shown in Fig. 1. Two-dimensional mechanical scanning of the animal along the transverse plane, in combination with time-resolved ultrasonic detection, provides volumetric resolution. Hence, no depth scanning is necessary.

To compare and validate OR-PAM with established fluorescence microscopy for imaging of amyloid

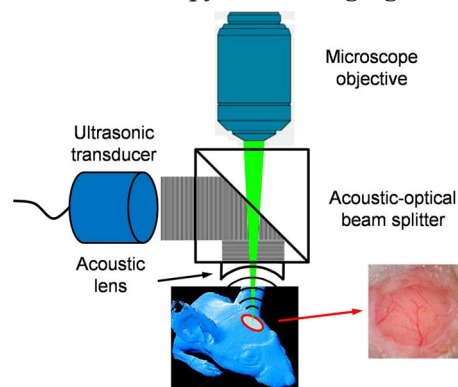


Fig. 1. (Color online) Schematic of the optical-resolution photoacoustic microscope for amyloid plaque imaging. OR-PAM imaging and multiphoton imaging were performed through a cranial window preparation (inset).

plaques, a Congo-red-stained brain section from a 10-month-old APP^{swe}/PS1^{dE9} mouse (APP/PS1, The Jackson Laboratory) was cover slipped and examined using a fluorescence microscope (BX50, Olympus) equipped with a MicroFire monochrome microscope digital CCD camera (Optronics) under Rhodamine excitation (496–540 nm). By measuring red fluorescence (520–625 nm), amyloid plaques were detected in APP/PS1 brain sections [Fig. 2(A)]. A 1 × 1 mm region of interest (ROI) (enclosed by the red dashed box in Fig. 2(A)), and replotted in Fig. 2(B) for better comparison) was imaged by OR-PAM using a 523 nm wavelength [Fig. 2(C)]. All amyloid plaques visualized using conventional fluorescence microscopy were observed with OR-PAM as well, suggesting that OR-PAM has the sensitivity and spatial resolution required to image amyloid plaques [a few representative plaques are paired up in Figs. 2(B) and 2(C) for comparison]. The main features of amyloid plaques in the two images were virtually identical (the correlation coefficient was calculated to be 0.95 based on both plaque size and location).

To examine the plaque imaging capability of OR-PAM in living mice, OR-PAM images were directly compared with the images acquired by multiphoton microscopy. A 10-month-old APP/PS1 mouse was injected with Congo red through the cisterna magna to label amyloid plaques *in vivo*. Twenty-four hours after injection, an open-skull cranial window covered by a plastic coverslip was created over the parietal cortex, and dye labeling was confirmed by conventional fluorescence imaging [Fig. 3(A)]. An ROI [enclosed by the red dashed box in Fig. 3(A)] containing a variety of amyloid plaques and blood vessels was selected for both dual-wavelength OR-PAM imaging and multiphoton imaging (LSM 510 META NLO system, Zeiss). Two-photon fluorescence was generated with 800 nm excitation (Chameleon Ti:sapphire laser, Coherent) and detected in the spectral range of 565–615 nm. A maximum-intensity-projection image [Fig. 3(B)] was generated by a *z*-stack image series acquired from the cranial window surface to a depth of ~200 μm into the cortex. The incremental *z*-step distance was 10 μm under a 10 \times water-immersion

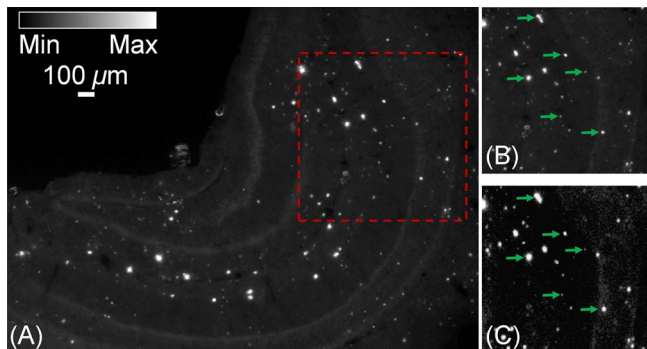


Fig. 2. (Color online) *In vitro* imaging of a Congo-red-stained brain section from a 10-month-old APP/PS1 mouse; (A) entire hippocampus imaged using conventional fluorescence microscopy; (B) region of interest selected from the boxed area in (A); (C) same region of interest imaged by OR-PAM for comparison. Arrows, plaques. Scale bar in (A) applies to all three parts.

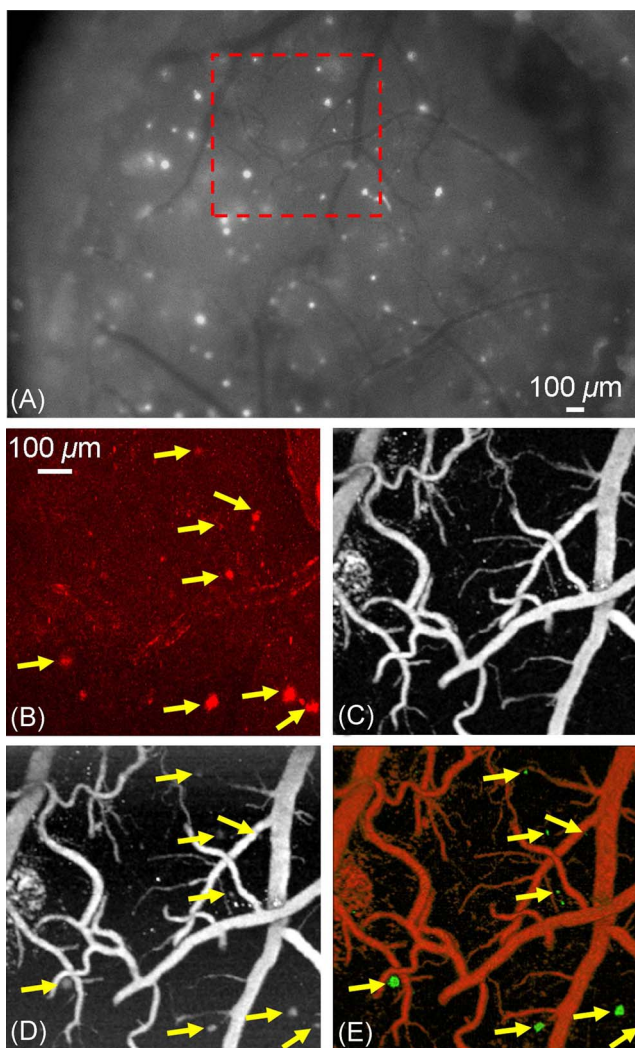


Fig. 3. (Color online) *In vivo* brain imaging of a Congo-red-injected 10-month-old APP/PS1 mouse through a cranial window. (A) Exposed cortical brain region imaged using conventional fluorescence microscopy through the cranial window. The region of interest marked by a red dashed box was imaged by multiphoton microscopy in (B), and OR-PAM at 570 nm in (C) and 523 nm in (D). (E) The processed dual-contrast OR-PAM image, where amyloid plaques are colored green (online) and blood vessels are colored red (online) [volumetric visualization is available online as (Media 1)]. Arrows, plaques. Scale bar in (B) applies to parts (B)–(E).

objective (NA 0.33, Zeiss). For the dual-wavelength OR-PAM imaging, optical wavelengths of 570 nm [Fig. 3(C)] and 523 nm [Fig. 3(D)] were selected to differentiate the photoacoustic signals generated by hemoglobin and Congo-red-labeled amyloid plaques. Imaging depths of amyloid plaques and blood vessels were quantified to be 230 μm and 450 μm from the cortical surface, respectively. The absorption of Congo red at 523 nm is ~6 times higher than that at 570 nm [4]; however, the absorption of hemoglobin differs by only 1.4 times [5]. Moreover, at each wavelength, the optical absorption coefficients of oxy- and deoxy-hemoglobin are nearly equal, so the blood photoacoustic signals reflect the total hemoglobin concentration regardless of the blood oxygenation level. Based on these two characteristics, the photoacoustic

image taken at 523 nm was linearly scaled to equalize the blood vessel signals with their counterparts taken at 570 nm, and then the two mutually normalized images were subtracted pixelwise to eliminate the blood signals and isolate the Congo-red-labeled amyloid plaques. Upon separating the distributions of the hemoglobin and the amyloid plaques, they were pseudocolored differently for clear visualization in both the maximum-amplitude-projection image [Fig. 3(E)] and the 3D movie (Media 1). Images acquired using OR-PAM and multiphoton microscopy were directly compared, revealing excellent correlation in plaque distribution [arrows, Figs. 3(B), 3(D), and 3(E)]. A few small plaques visualized using multiphoton microscopy [Fig. 3(B)] were not detected by the OR-PAM system [Fig. 3(E)], most likely owing to the limited signal-to-noise ratio caused by the nonoptimized excitation wavelength for Congo red detection and by the interference from the strong blood absorption. It should be noted that the imaged plaque sizes are slightly different as measured by the two imaging modalities. This likely reflects differences in imaging contrast and sensitivity between the two techniques; however, since each plaque can serve as its own control for time-lapsed imaging, measures of relative plaque growth are expected to be similar.

Although the current configuration of OR-PAM has successfully demonstrated the ability to image amyloid plaques *in vivo*, transcranial imaging (through an intact skull) is certainly more attractive for minimally invasive monitoring of AD progression and drug efficacy. OR-PAM has already been shown to be capable of imaging individual capillaries through intact skulls in living adult mice [6]. Thus *in vivo* transcranial OR-PAM imaging of amyloid plaques, which are similar to or larger than capillaries, is highly likely with further optimization of imaging parameters and improvements in the optical absorption of amyloid-specific dyes, as indicated below.

One possible improvement would take advantage of the fact that the absorption spectrum of Congo red peaks at 500–510 nm, where hemoglobin experiences a local absorption valley [4,5]. Downshifting the optical illumination wavelength of OR-PAM to 500–510 nm (not available in our current laser system) will increase the contrast between hemoglobin and Congo red by at least a factor of 4, which will help differentiate between amyloid plaques and blood vessels. Another possible improvement is to modify the current acoustic detection mechanism to avoid the unnecessary transformation of the photoacoustic signals from *p* waves to *sv* waves and to apply an ultrasonic anti-reflection coating to the acoustic lens. Still another improvement is suggested by the Fourier analysis of our transcranial mouse brain imaging data, which shows that decreasing the center frequency of the ultrasonic transducer from current 75 MHz to 40 MHz is expected to further increase the detected photoacoustic signals by twofold at the expense of spatial resolution.

Besides technical improvements to the OR-PAM system, developing amyloid-specific dyes absorbing

at the near-IR (NIR) optical window of biological tissues (700–800 nm) would be expected to further enhance *in vivo* amyloid plaque imaging [7]. Tissue scattering and absorption within the NIR range are greatly reduced compared with that in the visible spectrum. Working in the NIR region with the aid of highly specific amyloid dyes will allow deeper tissue penetration and provide higher contrast between the targeted amyloid plaques and the surrounding tissues.

Advances in the above aspects will likely allow OR-PAM imaging of amyloid plaques through an intact mouse skull. This noninvasive imaging capability will eliminate the influence of the cranial window preparations on the underlying brain tissues. Recent studies suggest that invasive cranial window preparations may adversely influence underlying brain tissue behavior [8,9]. Furthermore, imaging through an intact skull would greatly expand the available regions for imaging, thereby reducing the numbers of animals needed to quantify plaque growth. Such a model would be very attractive as an *in vivo* screen for drug development.

The authors appreciate Prof. James Ballard's close reading of the manuscript. This work was sponsored by National Institutes of Health (NIH) grants R01 NS48283, R01 NS67905, P01 NS32636 (J. M. L.), R01 EB000712, R01 NS46214, R01 EB008085, and U54 CA136398. L. V. W. has a financial interest in Microphotoacoustics, Inc. and Endra, Inc., which, however, did not support this work. For more information, contact J.-M. L. (animal model) or L. V. W. (photoacoustic imaging).

† Authors contributed equally to this work.

References

1. C. Wu, V. W. Pike, and Y. Wang, *Curr. Top. Dev. Biol.* **70**, 171 (2005).
2. W. E. Klunk, B. J. Bacsikai, C. A. Mathis, S. T. Kajdasz, M. E. McLellan, M. P. Frosch, M. L. Debnath, D. P. Holt, Y. Wang, and B. T. Hyman, *J. Neuropathol. Exp. Neurol.* **61**, 797 (2002).
3. S. Hu, K. Maslov, and L. V. Wang, *Med. Phys.* **36**, 2320 (2009).
4. C. L. Nie, X. S. Wang, Y. Liu, S. Perrett, and R. Q. He, *BMC Neurosci.* **8**, 9 (2007).
5. S. L. Jacques and S. A. Prahl, <http://omlc.ogi.edu/spectra/hemoglobin/index.html>, retrieved November 16, 2009.
6. S. Hu, K. Maslov, V. Tsytarev, and L. V. Wang, *J. Biomed. Opt.* **14**, 040503 (2009).
7. M. Hintersteiner, A. Enz, P. Frey, A. L. Jatton, W. Kinzy, R. Kneuer, U. Neumann, M. Rudin, M. Staufenbiel, M. Stoeckli, K. H. Wiederhold, and H. U. Gremlich, *Nat. Biotechnol.* **23**, 577 (2005).
8. H. T. Xu, F. Pan, G. Yang, and W. B. Gan, *Nat. Neurosci.* **10**, 549 (2007).
9. P. Yan, A. W. Bero, J. R. Cirrito, Q. Xiao, X. Hu, Y. Wang, E. Gonzales, D. M. Holtzman, and J. M. Lee, *J. Neurosci.* **29**, 10706 (2009).